Quantitative Finance and Economics

QFE, 9(4): 713–744.
DOI: 10.3934/QFE.2025025
Received: 21 April 2025
Revised: 23 June 2025
Accepted: 02 July 2025
Published: 01 October 2025

https://www.aimspress.com/journal/QFE

*Research article*

# A fractal market perspective on improving futures pricing and optimizing cash-and-carry arbitrage strategies

**Xu Wu and Yi Xiong***

School of Business Administration, Chengdu University of Technology, Xuefu Road 28, Chengdu, Sichuan 610059, P. R China

* **Correspondence:** Email: xiongyiemail@yeah.net; Tel: +8615015538960.

**Abstract:** Traditional futures pricing models, based on the efficient market hypothesis, often fail in today's complex financial markets, leading to significant pricing errors and unreliable arbitrage strategies. This study posits that the fractal market hypothesis (FMH) offers a superior framework by accounting for long memory and multi-scale dynamics. Methodologically, we developed a fractal futures pricing model by incorporating the Hurst exponent and constructed a novel cash-futures arbitrage strategy using trend fractal dimensions and momentum lifecycle logic to generate dynamic trading signals. Empirical analysis using CSI 300 data demonstrates that our fractal pricing model significantly reduces pricing errors compared to the traditional cost-of-carry model. Furthermore, the proposed fractal-based arbitrage strategy achieves substantially higher returns, superior risk-adjusted performance, and lower drawdowns than conventional threshold-based approaches, showing robustness across diverse market conditions. This research validates the practical value of FMH for developing more accurate pricing tools and more adaptive, profitable arbitrage strategies, offering valuable insights for investors and risk managers in nonlinear markets.

**Keywords:** fractal market hypothesis; futures pricing; cash-futures arbitrage; Hurst exponent; fractal dimension

**JEL Codes:** G12, G13, G14, C58

**Abbreviations:** ADF: Augmented Dickey–Fuller; AUM: Assets Under Management; BS: Black–Scholes; CFFEX: China Financial Futures Exchange; CoC: Cost-of-Carry; D+: Upward Trend

Fractal Dimension; D−: Downward Trend Fractal Dimension; DFA: Detrended Fluctuation Analysis; EMH: Efficient Market Hypothesis; ETF: Exchange Traded Fund; FBM: Fractional Brownian Motion; FMH: Fractal Market Hypothesis; FTD: Fractal Trend Dimension; GBM: Geometric Brownian Motion; H: Hurst exponent; J-B: Jarque–Bera; MAE: Mean Absolute Error; Max AE: Maximum Absolute Error; MF-DFA: Multifractal Detrended Fluctuation Analysis; MSE: Mean Squared Error; Q(20): Ljung-Box Q-statistic at lag 20; R/S: Rescaled Range

## 1. Introduction

The growing complexity of modern financial markets, exemplified by the proliferation of derivatives such as China's CSI 300 index futures, presents significant challenges to conventional financial theories. In the realm of futures pricing, the classical cost-of-carry model serves as a theoretical cornerstone (Cornell and French, 1983), its validity fundamentally predicated on the assumptions of the efficient market hypothesis (EMH) (Fama, 1970). The EMH posits market rationality and that asset prices follow a random walk. However, a vast body of empirical evidence reveals that real-world price dynamics are far more intricate, exhibiting well-documented "stylized facts" such as fat tails, volatility clustering, and, critically, long-range memory or persistence (Cont, 2001; Lo, 2004). These characteristics indicate that price movements are not independent events, but are shaped by a confluence of behavioral biases, limits to arbitrage (Chu et al., 2017), and market microstructure effects (Lucas, 2022; Nadtochiy, 2020; Bian et al., 2022). Consequently, traditional models that neglect the market's inherent fractal nature and memory (Peters, 1989) often generate significant pricing errors, undermining their reliability as valuation tools and impairing the efficacy of strategies like cash-and-carry arbitrage. This pronounced disconnect between theory and reality necessitates the pursuit of novel frameworks capable of endogenously capturing the market's long-term memory and complex dynamics.

In the field of asset pricing, recent developments in fractional models have offered new perspectives for understanding and predicting financial asset prices. In particular, the application of fractional Brownian motion (FBM), a concept first defined in the 1960s (Mandelbrot, 1963), has been extensively studied for its mathematical viability in finance. This pursuit has led to models that explicitly account for long-range dependence, not only in asset prices but also in their volatility, with seminal work showing that shocks to stock market volatility dissipate at a slow, hyperbolic rate best described by fractionally integrated processes (Bollerslev and Mikkelsen, 1996). Building on this foundation, researchers have re-engineered core financial theories, such as the development of a fractional-moment capital asset pricing model designed to be robust during periods of market panic when returns follow heavy-tailed distributions (Li et al., 2009). Further theoretical work has explored how FBM can be integrated into dynamic asset pricing frameworks, with studies demonstrating that its higher-order moments can influence agent decision-making without disrupting the underlying model structure (Yan and Wang, 2022). The practical superiority of these models has been validated empirically; for instance, the geometric fractional Brownian motion (GFBM) model has been shown to be more accurate than the traditional geometric Brownian motion (GBM) in simulating commodity price paths (Ibrahim et al., 2020). This enhanced descriptive power is particularly critical for the valuation of derivatives. Researchers have successfully developed pricing formulas for complex instruments like convertible bonds (Miao and Yang, 2015) and options under uncertain

fractional volatility (Gong et al., 2024), underscoring the positive outlook for using fractal models to minimize financial risks associated with derivatives (de Conti et al., 2021).

Concurrently, nonlinear asset pricing frameworks hold significant importance. Nonlinear asset pricing theories challenge the assumptions of traditional linear models, such as the capital asset pricing model (CAPM) (Lintner, 1965), by positing that the relationship between asset returns and risk factors is not linear. This recognition is critical, as recent research demonstrates that even sophisticated long-run risk models exhibit significant higher-order effects and nonlinearities, showing that common linear approximations can lead to considerable errors in predicting asset price dynamics (Pohl et al, 2018). This has spurred the development of advanced mathematical tools, such as nonlinear and nonlocal partial integro-differential equations used to price assets in markets with features like jumps and illiquidity (Yousuf and Khaliq, 2021). This line of research continues to evolve, with recent models demonstrating how interactions among heterogeneous agents—including fundamentalists, chartists, and imitators—can endogenously generate intricate bull and bear price dynamics and other complex market behaviors (Brianzoni and Campisi, 2020). On the other hand, the increasing availability of vast datasets has spurred the rise of powerful data-driven methods. Cutting-edge research now applies deep learning to this domain, constructing nonlinear asset pricing models with deep neural networks that excel at capturing complex, latent features and dynamic patterns in asset returns without imposing strong a priori structural assumptions (Dossatayev, 2024; Li et al., 2024; Yu and Yan, 2019; Kanzari and Said, 2023).

These theoretical advancements have direct and profound implications for practical trading strategies, most notably cash-and-carry arbitrage. As a cornerstone of derivatives trading, this strategy seeks to profit from temporary mispricings between a futures contract and its underlying spot asset, based on the principle that their prices should converge at the contract's expiration. In theory, an arbitrage opportunity exists whenever the observed basis deviates from the fair value dictated by carrying costs. However, the execution of this seemingly risk-free strategy is fraught with challenges, including transaction costs, market frictions, and, critically, the risk of model error. If the underlying pricing model is flawed—failing to account for the market's memory or nonlinear dynamics as discussed previously—then a perceived arbitrage window may be illusory, leading to persistent or widening spreads and unexpected losses. Consequently, modern approaches to arbitrage have evolved from simple threshold-based rules to more sophisticated statistical arbitrage methods. Among these, cointegration analysis (Engle and Granger, 1987) has become a standard tool to verify the existence of a stable, long-run equilibrium between spot and futures series (Chiu and Wong, 2011). However, the explanatory power of standard cointegration models is fundamentally limited. Its primary function is to confirm if a long-run equilibrium exists, typically by assuming that the speed of reversion back to the mean is a simple, constant parameter. In practice, the arbitrage basis rarely reverts in such a linear fashion. The process is often far more complex: the basis can exhibit periods of strong persistence, where it trends away from its fair value for extended durations, followed by episodes of rapid, anti-persistent reversion. This time-varying dynamic—where the strength and even direction of the relationship change—is precisely what linear models struggle to capture.

This observation opens a new avenue for analysis. Instead of treating the basis as a series that simply reverts to a mean, this research posits that incorporating FMH insights can significantly improve both futures pricing and cash-futures arbitrage strategies. By acknowledging and quantifying the market's fractal nature, particularly long-term memory, we can refine the traditional pricing framework. Specifically, this study proposes embedding the Hurst exponent into the futures

pricing formula (Aslam et al., 2020; Miloș et al., 2020; Jiang et al., 2019), reasoning that the long memory characteristic (H) directly influences the expected path and volatility dynamics of the underlying asset's price—core inputs to any forward-looking pricing model. A fractal-adjusted model should therefore provide a more accurate reflection of complex price evolution compared to the memoryless assumption of the cost-of-carry model, potentially reducing pricing errors. Building upon this improved pricing foundation, the study further explores optimizing cash-futures arbitrage through the lens of FMH. Traditional arbitrage relies on fixed basis thresholds derived from the cost-of-carry model, but the basis itself is a complex, nonlinear time series. FMH offers tools for more effective analysis. This research specifically leverages trend fractal dimensions (FTD), distinguishing between upward ($D^+$) and downward ($D^-$) dimensions, combined with momentum lifecycle theory (Wu et al., 2018). By analyzing the interplay between $D^+$ and $D^-$, we can potentially identify different phases in the basis's movement, such as trending momentum or potential reversal points. Designing an arbitrage strategy that dynamically adjusts entry and exit signals based on these identified fractal momentum phases, particularly focusing on capturing reversals, may offer superior performance compared to static methods by adapting more effectively to the market's multi-scale fluctuations and nonlinear behavior.

Therefore, the primary objectives of this study are threefold: first, to empirically investigate the presence and nature of fractal characteristics (long memory and multifractality) in the Chinese A-share market, using CSI 300 index ETF and futures data via robust methods like multifractal detrended fluctuation analysis (Kantelhardt et al., 2002). Second, based on these findings and FMH principles, to construct and rigorously evaluate a modified futures pricing model incorporating the Hurst exponent against the traditional cost-of-carry model using historical data and appropriate error metrics. Third, to design and empirically test an optimized cash-futures arbitrage strategy utilizing trend fractal dimensions and momentum lifecycle logic for dynamic signals, comparing its performance comprehensively (return, risk-adjusted return, drawdown, robustness) against a traditional static threshold strategy. To achieve these objectives, this research employs theoretical derivation, advanced fractal statistical analysis, econometric modeling, and rigorous empirical backtesting using high-frequency data from the CSI 300 index ETF and futures markets, consistently applying a comparative framework.

This study contributes significantly by advancing the application of FMH to futures pricing and arbitrage, offering a refined pricing model accounting for long memory and a dynamic arbitrage strategy grounded in multi-scale fractal analysis. It provides empirical evidence from China's CSI 300 market supporting the relevance of fractal dynamics in derivatives. Practically, it offers potentially more accurate pricing tools and more effective, robust arbitrage strategies for practitioners in complex markets, with implications for regulators monitoring market dynamics. The results presented demonstrate that the research aims—improving futures pricing accuracy and optimizing cash-futures arbitrage performance using a fractal market perspective—were successfully achieved. The remainder of this paper details the methodology (Section 2), describes the data and construction of price series (Section 3), and presents the empirical results, including fractal analysis, pricing model evaluation, and arbitrage strategy backtesting (Section 4). Finally, Section 5 summarizes findings, discusses implications, and suggests future research directions.

## 2. Methodology

### *2.1. Fractal market test*

To rigorously investigate the potential fractal nature and complex dynamics of the selected financial time series (CSI 300 ETF and its corresponding futures), departing from the traditional assumptions of market efficiency and random walks, this study employs MF-DFA methodology. Originally proposed by Kantelhardt et al. (2002), MF-DFA is a powerful and widely recognized technique particularly well-suited for analyzing nonstationary time series, which are characteristic of financial markets. Its key advantage lies in its ability to reliably detect long-range correlations (memory effects) while simultaneously characterizing the multifractal structure, meaning it can quantify how scaling properties vary across different magnitudes of fluctuations. This provides a much richer description of market dynamics than simpler monofractal approaches like standard DFA or R/S analysis. The procedure involves the following steps:

First, for a given time series $\{x_i\}$ of length $N$, we compute a cumulative sum series $Y(k)$. This step integrates the original signal and helps to transform potentially stationary fluctuations into a random walk–like process if the original series were uncorrelated. The profile is calculated by subtracting the mean $\bar{x}$ of the series and summing the deviations:

$$Y(k) = \sum_{i=1}^{k} (x_i - \bar{x}), \quad \text{for } k = 1, \ldots, N \tag{1}$$

Second, the integrated profile series $Y(k)$ is divided into $N_s \equiv \text{int}(N/s)$ non-overlapping segments of equal length (scale) $s$. Since the total length $N$ may not be an exact multiple of $s$, a similar procedure is repeated starting from the end of the series to ensure that all data points are utilized, resulting in a total of $2N_s$ segments. Within each segment $v$ (where $v$ ranges from 1 to $2N_s$), a local trend is estimated and removed. This detrending step is crucial for financial data as it eliminates polynomial trends (e.g., linear drifts or quadratic trends) that could otherwise contaminate the analysis of intrinsic fluctuations and potentially lead to spurious detection of long-range correlations. A polynomial function $p_v(i)$ of order m is fitted to the data within each segment using the least squares method. For many financial applications, a linear trend (m = 1) or quadratic trend (m = 2) is sufficient; in this study, we utilize a linear trend (m = 1) for detrending.

Third, after removing the local trend $p_v(i)$ in each segment $v$, the variance (mean square fluctuation) around the trend is calculated for that segment at scale $s$:

$$F^2(s,v) = \frac{1}{s} \sum_{i=1}^{s} \left[ Y((v-1)s + i) - p_v(i) \right]^2, \quad \text{for } v = 1, \ldots, Ns \tag{2}$$

A similar calculation is performed for segments $v = N_s + 1 \ldots 2N_s$, adjusting the indexing for the backward pass. This $F^2(s,v)$ quantifies the magnitude of detrended fluctuations within a specific segment $v$ at a given time scale $s$.

Fourth, the overall q-th order fluctuation function, $F_q(s)$, is obtained by averaging the segment variances $F^2(s,v)$ across all $2N_s$ segments. The parameter $q$ acts as a weighting exponent, allowing the analysis to differentiate between the scaling behaviors of small and large fluctuations. For $q \neq 0$, the fluctuation function is defined as:

$$F_q(s) = \left[ \frac{1}{2N_s} \sum_{v=1}^{2N_s} (F^2(s,v))^{q/2} \right]^{1/q} \tag{3}$$

Positive values of $q$ magnify the contribution of segments with large fluctuations (high volatility periods), while negative values of $q$ emphasize segments with small fluctuations (low volatility periods). The standard DFA corresponds to the case $q = 2$. For the special case $q = 0$, a logarithmic averaging is employed to avoid issues with potential zero values and to provide a balanced weighting:

$$F_0(s) = \exp\left[ \frac{1}{4N_s} \sum_{v=1}^{2N_s} \ln(F^2(s,v)) \right] \tag{4}$$

Finally, the scaling properties of the time series are examined by analyzing the relationship between the fluctuation function $F_q(s)$ and the time scale $s$. If the time series exhibits fractal scaling properties, $F_q(s)$ is expected to follow a power-law relationship with $s$:

$$F_q(s) \propto s^{h(q)} \tag{5}$$

The exponent $h(q)$ is the generalized Hurst exponent. It can be estimated as the slope of the linear regression of $\log(F_q(s))$ versus $\log(s)$ over a suitable range of scales $s$. If $h(q)$ is independent of $q$, the series is monofractal, characterized by a single scaling exponent [the Hurst exponent $H = h(2)$]. However, if $h(q)$ varies significantly with $q$, the time series is multifractal, indicating a more complex scaling structure where different fluctuation magnitudes scale differently. The value $h(2)$ specifically characterizes the long-range dependence: $h(2) > 0.5$ indicates persistent behavior, where past trends are likely to continue; $h(2) = 0.5$ signifies an uncorrelated random process; and $h(2) < 0.5$ implies anti-persistent behavior, where trends are likely to reverse.

### *2.2. Construction of the fractal futures pricing model*

#### 2.2.1. Review of the traditional futures pricing formula

Futures pricing represents a cornerstone in the valuation of financial derivatives, and understanding its underlying mechanisms remains a central theme in financial research. Traditional approaches to futures pricing are primarily anchored in the no-arbitrage principle and the dynamics of the underlying spot market price. Among these, the cost-of-carry model stands out as the most widely applied framework. This model posits that the futures price is determined by the current spot price, the costs associated with holding the underlying asset (including storage fees, interest costs,

etc.), and any income or yield generated during the holding period. The fundamental formula for the cost-of-carry model is expressed as:

$$F_t = S_t \times e^{(r-q)(T-t)} \tag{6}$$

where $F(t,T)$ denotes the futures price at time $t$ for a contract maturing at time $T$, $S(t)$ is the spot price at time $t$, $r$ represents the risk-free interest rate, $q$ is the continuous yield generated by the underlying asset during the holding period (such as dividend yield for stock indices or convenience yield for commodities), and $(T-t)$ signifies the time remaining until the contract's expiration.

The derivation of this formula relies on several critical assumptions. The foremost assumption is the absence of risk-free arbitrage opportunities within the market, precluding investors from securing guaranteed profits without risk by simultaneously trading in the spot and futures markets (or vice versa). Secondly, the spot price of the underlying asset is typically assumed to follow a geometric Brownian motion (GBM), mathematically represented by the stochastic differential equation:

$$dS_t = \mu S_t dt + \sigma S_t dW_t \tag{7}$$

where $\mu$ is the expected rate of return of the asset, $\sigma$ represents its volatility, and $dW(t)$ is the increment of a standard Brownian motion (Wiener process). Further assumptions include the absence of transaction costs and taxes, simplifying the trading environment. Lastly, the model presupposes a frictionless and continuously divisible market, where participants can trade any fraction of an asset at any point in time without impediment.

Under these stipulated conditions, constructing a theoretical no-arbitrage portfolio and applying mathematical tools such as Itô's lemma allows for the derivation of the relationship between futures and spot prices, culminating in the aforementioned cost-of-carry formula. This model provides significant practical guidance and holds substantial importance in real-world applications. However, its foundation rests upon the assumption that the market follows a memoryless Brownian motion, implying that price fluctuations possess independent and identically distributed characteristics. These assumptions often fail to hold completely in actual market conditions, particularly when markets exhibit complex dynamics and nonlinear features.

Empirical research has increasingly demonstrated that financial markets display more intricate dynamic characteristics than captured by traditional models. Features such as self-similarity and long-range dependence (long memory) are often observed in financial time series, indicating that past price movements can influence future fluctuations over extended periods. These characteristics fundamentally deviate from the random walk hypothesis inherent in the GBM framework used by the traditional cost-of-carry model. Consequently, the traditional model's capacity to fully capture these complex dynamics is inherently limited, potentially leading to inaccuracies in pricing, especially in markets characterized by significant complexity and nonlinearity.

### 2.2.2. Derivation of the fractal futures pricing formula

Fractal market theory, originating from Mandelbrot's (1963) research on the fractal structure of market price series, posits that traditional Brownian motion is insufficient to explain the long memory and self-similarity characteristics exhibited by certain financial time series. To address this,

fractional Brownian motion (FBM), characterized by the Hurst exponent $H \in (0,1)$, is introduced to provide a more flexible depiction of price fluctuations. Its primary properties include:

• Self-similarity: For any constant $\lambda > 0$, $B_{\lambda t}^H$ and $\lambda^H B_t^H$ have the same distribution, denoted as:

$$B_{\lambda t}^H \overset{d}{=} \lambda^H B_t^H \tag{8}$$

where H denotes the Hurst index, $B_t^H$ denotes the value of fractional Brownian motion at time point t, and $\overset{d}{=}$ denotes equal in distribution.

• Long memory or short memory: If $H > 0.5$, FBM exhibits long-range positive correlation (persistence). If $H = 0.5$, it degenerates into standard Brownian motion (no memory). If $H < 0.5$, it exhibits negative autocorrelation (anti-persistence).

• Gaussianity: For any time $t$, $B_H(t)$ is a Gaussian random variable with $E\left[B_H(t)\right] = 0$ and $Var[B_H(t)] = t^{2H}$.

However, FBM is not a semimartingale in the classical sense (for $H \neq 0$); consequently, tools such as Itô's lemma and the Girsanov theorem cannot be directly applied to construct a rigorous arbitrage-free pricing framework. Therefore, constructing an approximate fractal risk-neutral measure, aiming to derive a pricing framework analogous to Black–Scholes, becomes a central proposition of this study. Specifically, adopting a martingale approach, this paper potentially utilizes concepts related to fractal discounting or modified price processes to ensure that a suitably discounted price process approximates the martingale property under the constructed measure.

In the classic Black–Scholes framework, under the risk-neutral measure $Q$, the drift of the asset price $S(t)$ is adjusted to $(r-q)$, where $r$ is the risk-free rate, and $q$ is the dividend yield or convenience yield. The discounted process $e^{-\int_0^t (r-q)ds} S(t)$ then becomes a martingale, allowing for the derivation of the familiar futures pricing formula. However, once standard Brownian motion is replaced with FBM exhibiting long memory, this structure loses its theoretical rigor. Traditional risk-neutral pricing tools are difficult to apply directly. Persisting with a standard discount factor fails to guarantee the martingale property and inadequately incorporates the mathematical representation of volatility adjustments arising from "self-similar memory". In essence, the classical discount factor does not fully accommodate fractal market characteristics, thus failing to inherently introduce fractal correction terms into futures pricing.

To reconcile fractal dynamics with approximate arbitrage-free pricing, this study explores modifications to the standard framework. One conceptual avenue involves adjusting the drift or the discount factor itself. We consider a modified log-price process under a measure $Q$, with the aim of achieving an approximate martingale property for the discounted price. Let the logarithmic process of the underlying asset price $S(t)$ under $Q$ be modeled as:

$$\mathrm{d}(\log S(t)) = \left(\mu - \frac{1}{2}\sigma^2\right)\mathrm{d}t + \sigma \mathrm{d}B_H(t) \tag{9}$$

Here, $B_H(t)$ is the fractional Brownian motion with Hurst exponent $H$, $\sigma$ is the volatility parameter associated with the FBM noise, and $\mu$ is the drift under measure $Q$ that needs to be determined to ensure consistency with no-arbitrage principles (in an approximate sense). The standard no-arbitrage argument in the BS world leads to $(\mu - \frac{1}{2}\sigma^2 = r - q)$. We adapt this intuition for the FBM context.

Based on the goal of achieving a pricing formula consistent with no-arbitrage ideas in the fractal setting, we posit that under the approximate risk-neutral measure $Q$, the appropriate drift aligns with the risk-free rate adjusted for payouts, leading to the following log-price process under $Q$:

$$\mathrm{d}(\log S(t)) = (r - q)\mathrm{d}t + \sigma \mathrm{d}B_H(t) \tag{10}$$

This specification is a key step, effectively assuming that the expected rate of return under the pricing measure $Q$ is the risk-adjusted rate $(r - q)$, while the stochastic component is driven by FBM. The justification for this specific form, particularly the absence of an explicit FBM-related drift adjustment term often found in rigorous FBM models, is based on seeking a tractable model that extends BS naturally while incorporating the fractal variance structure. This simplification facilitates derivation while capturing the core impact of the Hurst exponent through the variance term.

Based on this log-price process under $Q$, the futures price $F(t,T)$ for delivery at time $T$, viewed from time $t$, is given by the conditional expectation:

$$F(t,T) = E^Q[S(T)|\ \mathcal{F}_t] \tag{11}$$

We can express $S(T)$ in terms of $S(t)$ using the assumed log-price dynamics:

$$S(T) = S(t)\exp\left(\int_t^T (r - q)ds + \int_t^T \sigma dB_H(s)\right) \tag{12}$$

$$S(T) = S(t)\exp\big((r - q)(T - t) + \sigma(B_H(T) - B_H(t))\big) \tag{13}$$

Substituting this into the expectation:

$$F(t,T) = E^Q\left[S(t)\exp\big((r - q)(T - t) + \sigma(B_H(T) - B_H(t))\big)|\ \mathcal{F}_t\right] \tag{14}$$

Since $S(t)$ and $(r - q)(T - t)$ are known at time t (belong to the filtration $F_t$):

$$F(t,T) = S(t)\exp\big((r - q)(T - t)\big)E^Q\left[\exp\big(\sigma(B_H(T) - B_H(t))\big)|\ \mathcal{F}_t\right] \tag{15}$$

The increment $B_H(T) - B_H(t)$ is a Gaussian random variable. While its distribution conditional on $F_t$ can be complex for $H \neq 0.5$ due to dependence, a common simplification or result from specific FBM pricing approaches (like those related to Wick calculus or assuming that conditional expectation simplifies appropriately) uses its unconditional distribution properties. The variable

σ(BH(T)−BH(t)) is Gaussian with mean 0. Its variance is $\sigma^2 \mathrm{Var}(B_H(T)-B_H(t))$. The exact variance is $\sigma^2 |T-t|^{2H}$. However, many FBM pricing models employ an approximation or result related to the variance structure, leading to the use of $T^{2H}-t^{2H}$ within the exponential term of the pricing formula. Following the convention adopted in the source text:

$$E^{Q}\left[\exp\left(\sigma(B_H(T)-B_H(t))\right)\right] \approx \exp\left(\frac{1}{2}\sigma^2(T^{2H}-t^{2H})\right) \tag{16}$$

Substituting this yields the fractal futures pricing formula:

$$F(t,T) = S(t)\exp\left((r-q)(T-t)+\frac{1}{2}\sigma^2(T^{2H}-t^{2H})\right) \tag{17}$$

This derivation relies on the assumed log-price process under $Q$ and the specific form used for the expectation involving the FBM variance. The choice of the drift $(r-q)$ in the log-price process under $Q$ is a crucial simplifying assumption, analogous to setting the parameter $\theta$ (related to potential FBM drift corrections in a more complex derivation) to zero, justified by:

(1) Correspondence with classic BS: When $H=0.5$, $T^{2H}-t^{2H}=T-t$. The term $\frac{1}{2}\sigma^2(T-t)$ corresponds to the variance part in the log-normal expectation. The resulting formula aligns conceptually with BS principles, although the standard BS futures price $F=Se^{(r-q)(T-t)}$ arises because the $\frac{1}{2}\sigma^2$ term in the drift cancels the $\frac{1}{2}\sigma^2$ term from the variance in the expectation $E[S(T)]$. Here, the fractal term remains.

(2) Simplicity: Assuming the drift under $Q$ is simply $(r-q)$ leads to a tractable model where the fractal nature primarily enters through the variance structure $T^{2H}-t^{2H}$.

(3) Intuition: The resulting formula $F(t,T) = S(t)\exp\left((r-q)(T-t)+\frac{1}{2}\sigma^2(T^{2H}-t^{2H})\right)$ clearly separates the standard cost-of-carry component from a fractal volatility adjustment term.

In summary, by assuming a specific log-price process driven by FBM under an approximate risk-neutral measure $Q$, motivated by extending the BS framework and seeking tractability, we arrive at the following fractal futures pricing formula:

$$F(t,T) = S(t)\exp\left((r-q)(T-t)+\frac{1}{2}\sigma^2(T^{2H}-t^{2H})\right) \tag{18}$$

This pricing formula explicitly incorporates a "fractal correction term", $\frac{1}{2}\sigma^2(T^{2H}-t^{2H})$, into futures pricing, reflecting the market's self-similar memory effect through the Hurst exponent H. Based on different values of H, the following interpretations can be derived:

If $H=0.5$, the formula reflects characteristics similar to the Black–Scholes world, though the exact BS formula $F=Se^{(r-q)(T-t)}$ requires the drift adjustment and variance term to precisely cancel in the expectation of S(T). The derived formula retains a variance term $\frac{1}{2}\sigma^2(T-t)$.

If $H > 0.5$, it indicates a strong positive correlation (long memory) in the market. The term $(T^{2H} - t^{2H})$ grows faster with time-to-maturity $(T-t)$ compared to the $H = 0.5$ case, suggesting that futures prices might be more sensitive to volatility over longer horizons due to persistence.

If $H < 0.5$, it suggests negative correlation (anti-persistence or mean reversion). The growth of $(T^{2H} - t^{2H})$ with $(T-t)$ is slower than for $H = 0.5$, implying market shocks tend to be reversed more quickly, potentially leading to different term structures or volatility sensitivities compared to the persistent case.

### *2.3. Construction of the fractal cash-futures arbitrage strategy*

Building upon the fractal market hypothesis and the derived fractal pricing insights, we propose an enhanced cash-futures arbitrage strategy. This strategy incorporates the fractal trend dimension (FTD) and momentum lifecycle theory to refine the identification and execution of arbitrage opportunities based on the behavior of the basis (the difference between spot and futures prices, $Basis_t = S_t - F_t$).

#### 2.3.1. Fractal trend dimension (FTD)

While a standard fractal dimension measures the overall complexity of a series, the FTD provides a more nuanced view by specifically distinguishing the fractal characteristics of upward and downward price movements. This is achieved by calculating separate fractal dimensions for ascending trends ($D^+$) and descending trends ($D^-$).

The calculation procedure involves defining the total length $L(R)$, upward trend length $L^+(R)$, and downward trend length $L^-(R)$ of the basis time series $\{P_i\}$ at various scales $R$:

$$L(R) = \sum \frac{|P_{i+1} - P_i|}{R} \tag{19}$$

$$L^+(R) = \sum \frac{\max(P_{i+1} - P_i, 0)}{R} \tag{20}$$

$$L^-(R) = \sum \frac{\max(P_i - P_{i+1}, 0)}{R} \tag{21}$$

These lengths are assumed to follow power-law relationships with the scale R:

$$L(R) \propto R^{1-D} \tag{22}$$

$$L^+(R) \propto R^{1-D^+} \tag{23}$$

$$L^{-}(R) \propto R^{1-D^{-}} \tag{24}$$

The fractal dimensions $D$, $D^{+}$, and $D^{-}$ are then estimated by performing linear regressions on the log-log plots of $L$, $L^{+}$, and $L^{-}$ against $R$, respectively.

### 2.3.2. Momentum lifecycle identification

Based on the work of Wu et al. (2018), the interplay between the overall fractal dimension ($D$), the upward trend dimension ($D+$), and the downward trend dimension ($D-$) for the basis series can be used to identify the current stage of its momentum lifecycle. These stages, which include upward momentum, downward momentum, high reversal, and low reversal phases, provide signals for constructing our arbitrage strategy. The specific conditions for each phase are defined as follows:

- The basis is considered in the downward momentum phase when $D^{-} \le D$ and $D^{-} < 1.5$, or $1.5 > D^{+} \ge D$, or $D^{+} = 0$.
- The basis is considered in the upward momentum phase when $D^{+} \le D$ and $D^{+} < 1.5$, or $1.5 > D^{-} \ge D$, or $D^{-} = 0$.
- The basis is considered in the low reversal phase when $D^{+} \ge D$ and $D^{+} > 1.5$, or $1.5 < D^{-} \le D$.
- The basis is considered in the high reversal phase when $D^{-} \ge D$ and $D^{-} > 1.5$, or $1.5 < D^{+} \le D$.

### 2.3.3. Trading strategy rules

To enhance the arbitrage strategy, focusing on potentially significant basis reversions and aiming to reduce unnecessary trades during established momentum phases, the trading signals are generated primarily during the identified reversal phases. Considering the goal of capturing basis convergence and constraints like short-selling restrictions in some markets (like the A-share market), this strategy prioritizes entering trades during the low reversal phase and exiting/potentially reversing during the high reversal phase.

The core trading rules are defined as:

- Rule 1: Execute a positive arbitrage (sell futures, buy spot/ETF) when the basis series enters the low reversal phase, as identified by the conditions on $D^{+}$ and $D^{-}$.
- Rule 2: Close the positive arbitrage position (buy futures, sell spot/ETF) when the basis series enters the high reversal phase, as identified by the conditions on $D^{+}$ and $D^{-}$ (depending on market rules and strategy design, this phase could also trigger the entry of a negative arbitrage trade).

This approach leverages the insights from fractal trend analysis to time arbitrage entries and exits, aiming for improved performance compared to traditional strategies relying solely on fixed basis thresholds.

## 3. Data

### *3.1. Data sources*

The empirical analysis in this study aims to cover a significant period of the Chinese capital market, primarily extending up to December 31, 2024. The precise start date for analyses involving the chosen spot ETF is determined by its listing date, as detailed in Section 3.2, to ensure the availability of its complete trading history. This overall timeframe, spanning over a decade, comprehensively covers several crucial phases of the Chinese capital market. These include, but are not limited to, the significant stock market volatility in 2015, the circuit breaker mechanism in early 2016, the initial impacts of Sino-US trade frictions in 2018, and the global market turbulence triggered by the COVID-19 pandemic in early 2020. The inclusion of these major structural break events provides a robust basis for testing the resilience and performance of the proposed models and strategies under diverse market conditions.

The primary data frequency employed in this research is 5-minute intervals. This frequency captures intraday price dynamics while mitigating potential market microstructure noise associated with ultra-high-frequency data. All data were obtained from Wind Financial Terminal, iFinD, Choice Financial Terminal, JoinQuant, and Resset Financial Research Database.

### *3.2. Spot asset selection*

The underlying index for the futures contracts in this study is the CSI 300 Index. For implementing cash-futures arbitrage, a tradable instrument that accurately tracks this index is required as the spot component. ETFs tracking the CSI 300 Index serve this purpose. The selection of an appropriate ETF is critical, as factors like fund scale, liquidity, and tracking accuracy directly impact arbitrage efficiency and feasibility. Generally, larger fund scales are associated with higher liquidity and lower market impact costs, which is advantageous for executing arbitrage trades with minimal slippage.

Therefore, we screened for CSI 300 ETFs with significant assets under management (AUM). As of December 2, 2024, four ETFs tracking the CSI 300 Index exceeded RMB 100 billion in scale. These candidates are detailed in Table 1.

**Table 1.** CSI 300 ETFs with AUM Above RMB 100 billion.

| Fund code | Fund name | Fund scale (RMB billion) |
|---|---|---|
| 510300.SH | Huatai-PineBridge CSI 300 ETF | 3605.71 |
| 510310.SH | E Fund CSI 300 ETF | 2451.79 |
| 510330.SH | ChinaAMC CSI 300 ETF | 1630.98 |
| 159919.SZ | Harvest CSI 300 ETF | 1548.15 |

The analysis period for selecting the optimal ETF considers their full trading history up to December 2, 2024, to ensure complete daily closing price data availability for all four candidate ETFs during their respective lifespans.

To evaluate how well these ETFs track the underlying index, we calculated the correlation matrix of their daily returns against the CSI 300 Index returns. The results are presented in Table 2.

**Table 2.** Correlation matrix of daily returns.

| | Harvest CSI 300 ETF | Huatai-PineBridge CSI 300 ETF | E Fund CSI 300 ETF | ChinaAMC CSI 300 ETF | CSI 300 Index |
|---|---|---|---|---|---|
| Harvest CSI 300 ETF | 1.0000 | 0.9999 | 0.9999 | 0.9998 | 0.9998 |
| Huatai-PineBridge CSI 300 ETF | 0.9999 | 1.0000 | 0.9999 | 0.9997 | 0.9998 |
| E Fund CSI 300 ETF | 0.9999 | 0.9999 | 1.0000 | 0.9997 | 0.9998 |
| ChinaAMC CSI 300 ETF | 0.9998 | 0.9997 | 0.9997 | 1.0000 | 0.9995 |
| CSI 300 Index | 0.9998 | 0.9998 | 0.9998 | 0.9995 | 1.0000 |

The correlation coefficients are all extremely close to 1, confirming that all four ETFs exhibit excellent tracking performance relative to the CSI 300 Index.

Beyond correlation, we assessed the ETFs based on key risk and return metrics, including historical return, excess return, Sharpe ratio, standard deviation, Alpha, Beta, and tracking error. These metrics are summarized in Table 3.

**Table 3.** Risk and return profile of candidate ETFs.

| | Return | Excess return | Sharpe ratio | Std.Dev | Alpha | Beta | Tracking error |
|---|---|---|---|---|---|---|---|
| Harvest CSI 300 ETF | 12.12% | 8.44% | 7.35 | 1.38% | 1.69 | 1 | 0.0306 |
| Huatai-PineBridge CSI 300 ETF | 11.87% | 8.19% | 7.19 | 1.37% | 1.56 | 0.99 | 0.0303 |
| E Fund CSI 300 ETF | 12.64% | 8.96% | 7.76 | 1.37% | 2.08 | 1 | 0.0303 |
| ChinaAMC CSI 300 ETF | 12.51% | 8.83% | 7.63 | 1.38% | 2.00 | 0.99 | 0.0416 |
| CSI 300 Index | 3.68% | | 1.22 | 1.38% | | | |

Considering the fund scale, correlation analysis, and the risk/return profiles, the E Fund CSI 300 ETF (ticker: 510310.SH) was selected as the spot asset proxy for the arbitrage strategy. This ETF was listed on March 25, 2013. Therefore, data for this spot instrument and related analyses in this study commence from this date, extending up to December 31, 2024, as mentioned in Section 3.1. This decision is based on its superior combination of the highest historical return (12.64%), joint-lowest tracking error (0.0303), lowest standard deviation (1.37%), and a Beta of 1.00, indicating precise market movement tracking. These characteristics suggest it provides a robust and efficient instrument for the spot leg of the cash-futures arbitrage. Consistent with the overall data strategy outlined in Section 3.1, 5-minute frequency data for this ETF is used for the empirical analysis within this timeframe.

### *3.3. Futures contract selection and processing*

The futures component of this study involves the CSI 300 Index Futures contracts traded on the China Financial Futures Exchange (CFFEX). Derivative contracts possess a finite lifespan constrained by their maturity date. Consequently, when dealing with futures data spanning extended periods, it is essential to address the issue of data discontinuity arising from contract expirations. The construction of continuous time series is crucial for both academic research and trading purposes.

The core challenge in constructing a continuous futures series lies in managing the "rollover" from an expiring contract to the next one. Various rollover methodologies exist in practice, particularly concerning the choice of the specific rollover date (the point in time when switching from the front contract to the next) and whether to adjust for price gaps. However, research has investigated the impact of choosing different rollover methods. For instance, studies comparing continuous return series of stock index futures constructed using different methodologies have found that regardless of the criterion applied, there are no statistically significant differences between the resulting series (Carchano and Pardo, 2009). This finding suggests that employing the least complex rollover method can yield reliable research conclusions without necessitating intricate adjustment mechanisms. Furthermore, for certain applications, such as the arbitrage strategy analysis central to this study, directly reflecting the price dynamics of the most actively traded and liquid contract (often the front-month contract) is paramount. A simple splicing method effectively meets this requirement.

Based on these considerations—namely, that simplicity does not compromise the reliability of the results and that it allows for direct reflection of the most active contract's dynamics—this study adopts a straightforward and commonly used method to construct the continuous futures price series. The specific procedure is as follows: At any given time, we utilize the nearest-month contract exhibiting the highest liquidity. As this contract approaches its expiration date or enters the delivery month, the data series is rolled over to the next nearest-month contract that has subsequently become the most liquid. This rollover is achieved by directly splicing the price data from the new contract to continue the time series, without applying adjustments for potential price gaps between the two contracts at the rollover point.

Employing this rollover procedure, we constructed the continuous futures series using 5-minute interval data. To align with the availability of the chosen spot ETF data, this futures series spans the period from March 25, 2013, to December 31, 2024. This involved sequentially splicing the data from all relevant monthly CSI 300 Index Futures contracts traded on the CFFEX during this timeframe. After processing, this yielded an extensive high-frequency time series for the empirical analysis, ensuring a consistent dataset for comparison with the spot market and for the subsequent development and testing of our models and strategies.

## 4. Empirical results

### *4.1. Statistical properties and fractal analysis of returns*

#### 4.1.1. Preliminary analysis: stylized facts and stationarity

Before delving into the pricing models and arbitrage strategies, it is crucial to understand the statistical characteristics and underlying dynamics of the chosen spot ETF (E Fund CSI 300 ETF,

510310.SH) and the constructed continuous CSI 300 Index Futures contract. For this analysis, we utilize 5-minute frequency data for both the spot ETF and the continuous futures series, spanning from March 25, 2013, to December 31, 2024, as established in Section 3.

We begin by examining the descriptive statistics and distributional properties of the return series. Table 4 summarizes the key statistics, while Figure 1 presents the frequency histograms, and Figure 2 shows the normal probability (Q-Q) plots for both series.

**Table 4.** Descriptive statistics of spot and futures.

| | Std.Dev | Skewness | Kurtosis | J-B Statistic | Q(20) | ADF statistic |
|---|---|---|---|---|---|---|
| Spot ETF | 0.16% | 0.03 | 4.95 | 18517.49*** | 786.41*** | −370.28*** |
| Futures | 0.15% | 0.10 | 4.71 | 14383.09*** | 70.13*** | −343.34*** |

Note: *** denotes significance at the 1% level. J-B tests the null hypothesis of normality. Q(20) is the Ljung-Box statistic testing for autocorrelation up to lag 20. ADF tests the null hypothesis of a unit root.

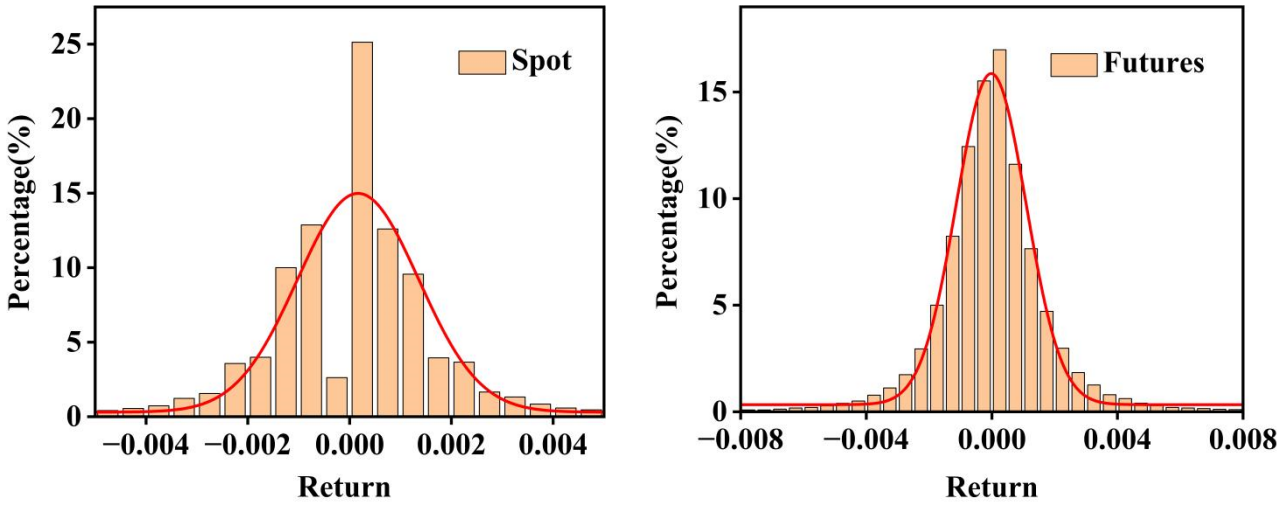


**Figure 1.** Frequency histograms of 5-minute returns for spot ETF and futures.

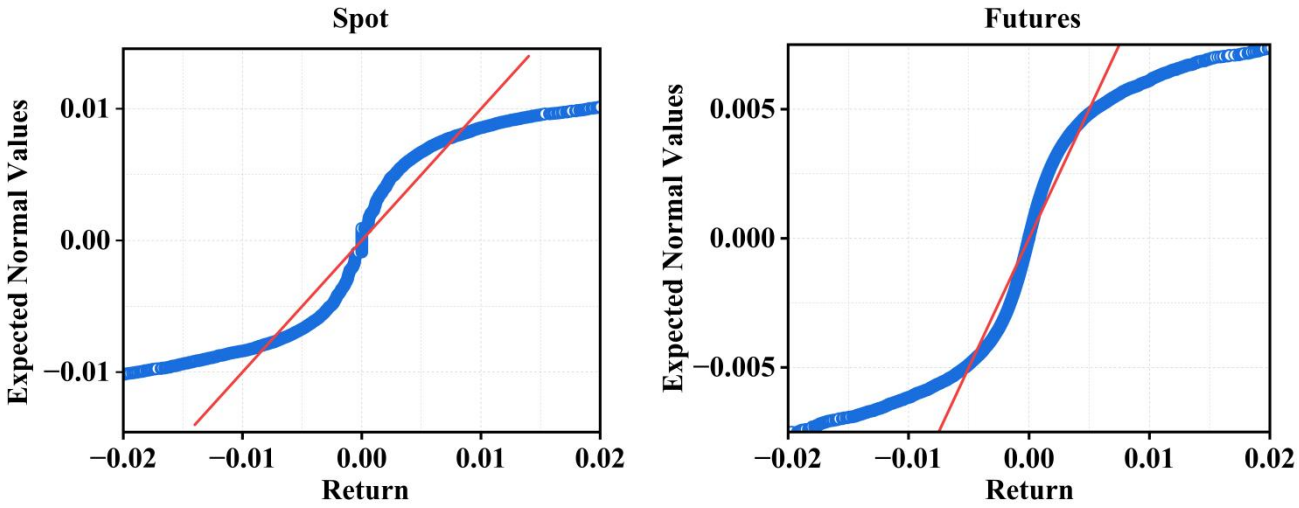


**Figure 2.** Normal probability plots of 5-minute returns for spot ETF and futures.

The results presented in Table 4 highlight significant departures from the standard assumptions of normality and independence that underpin many traditional financial models. The return series for both the spot ETF and futures display the classic stylized facts of financial data: they exhibit slight positive skewness (0.03 and 0.10, respectively) and pronounced leptokurtosis. With kurtosis values of 4.95 (spot) and 4.71 (futures) far exceeding the Gaussian benchmark of 3, the distributions are clearly *fat-tailed*. This characteristic, visually evident in the peaked histograms (Figure 1) and the S-shaped deviations in the Q-Q plots (Figure 2), confirms that extreme price movements occur much more frequently than a normal distribution would suggest. The extremely large and statistically significant J-B statistics (18517.49 and 14383.09) formally and emphatically reject the null hypothesis of normality for both series. Moreover, the significant Ljung-Box Q(20) statistics (786.41 for spot, 70.13 for futures) provide strong evidence against the independence of returns, indicating the presence of serial dependence or memory. Finally, the highly significant negative ADF test statistics (−370.28 and −343.34) confirm that both 5-minute return series are stationary, making them suitable for further time series analysis.

### 4.1.2. Multifractal analysis and long-range memory

Given these departures from normality and the evidence of serial dependence, we proceed to investigate the potential fractal nature of the return series using MF-DFA. This method is robust to nonstationarities and can effectively quantify long-range correlations and multifractality. We calculate the generalized Hurst exponent, h(q), over a range of orders q from −20 to 20. If the series is monofractal, h(q) will be constant; if it is multifractal, h(q) will vary with q. The results are presented in Figure 3.

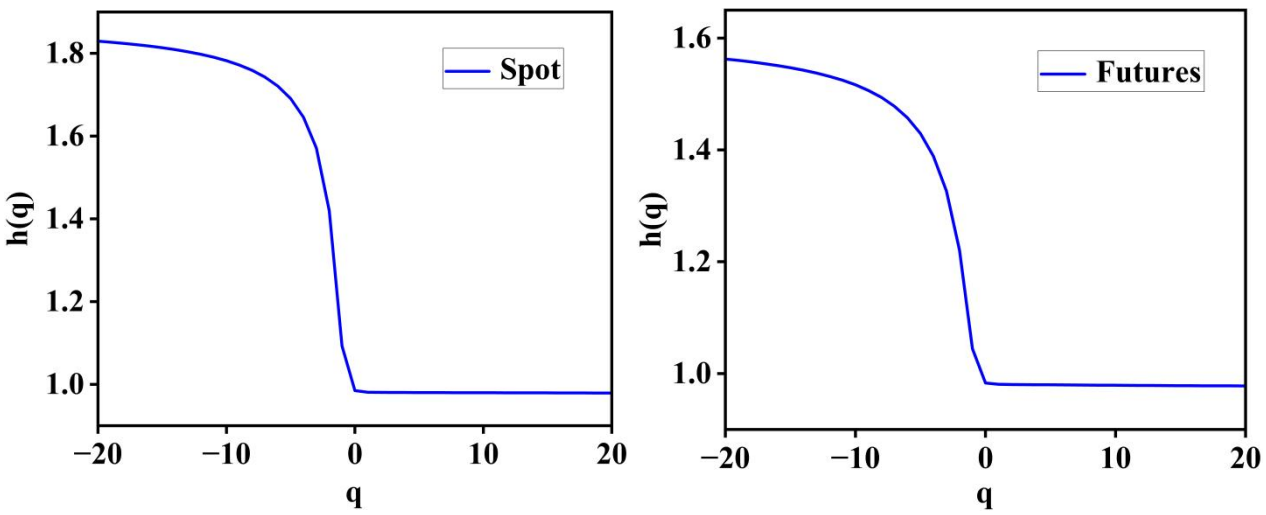


**Figure 3.** Generalized Hurst exponent h(q) as a function of q for 5-minute returns.

Figure 3 provides clear evidence supporting the fractal nature of the market returns. For both the spot ETF and futures series, the generalized Hurst exponent h(q) is not a constant but a distinctly decreasing function of q. This dependence is a hallmark of multifractality, indicating a complex scaling structure where the properties of small fluctuations (emphasized by negative q) differ from those of large fluctuations (emphasized by positive q). More critically for our study, the value of the

exponent at q = 2, commonly denoted as the Hurst exponent H, quantifies the long-range dependence. For both series, h(2) is significantly greater than the 0.5 benchmark for a random walk, indicating strong long-range positive correlations, or persistence. This means that periods of high (or low) volatility tend to be followed by more periods of high (or low) volatility, a memory effect not captured by traditional models.

#### 4.1.3. Robustness and validation of the Hurst exponent

To ensure the reliability of this crucial finding and refine the Hurst exponent estimate for use in our pricing model, we performed a comprehensive set of validation tests.

First, a scale-sensitivity analysis was conducted to confirm the stability of the MF-DFA estimate. Figure 4 displays the log-log plot of the fluctuation function versus the time scale for the futures returns (q = 2 shown as a representative case). The distinct and stable linear relationship over a wide range of intermediate and large scales confirms that power-law scaling is a genuine feature. The regression was carefully fitted to this linear region, excluding the smallest scales where market microstructure noise can distort the results, thus ensuring that the estimate reflects the true long-term memory of the process.

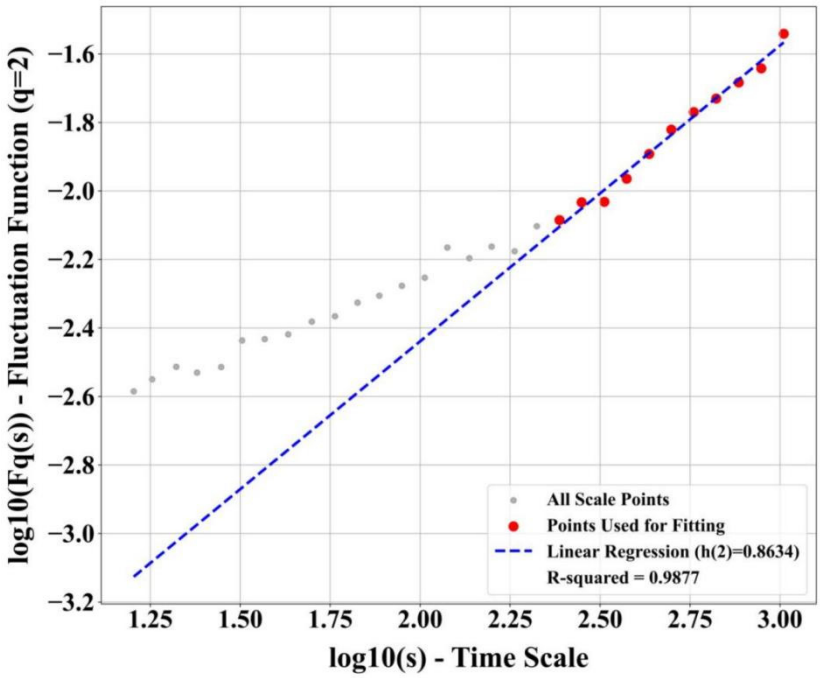


**Figure 4.** Log-log plot of the fluctuation function $F_q(s)$ against time scale s for futures returns.

Second, a sub-sample stability analysis was performed to ensure that high persistence was not an artifact of averaging over different market regimes. As shown in Figure 5, the Hurst exponent [h(2)] was calculated for numerous overlapping data segments of varying lengths. The estimates are remarkably consistent, with the vast majority falling in the highly persistent 0.80–0.95 range. This temporal robustness indicates that strong persistence is an intrinsic and enduring characteristic of the market's dynamics throughout our sample period.

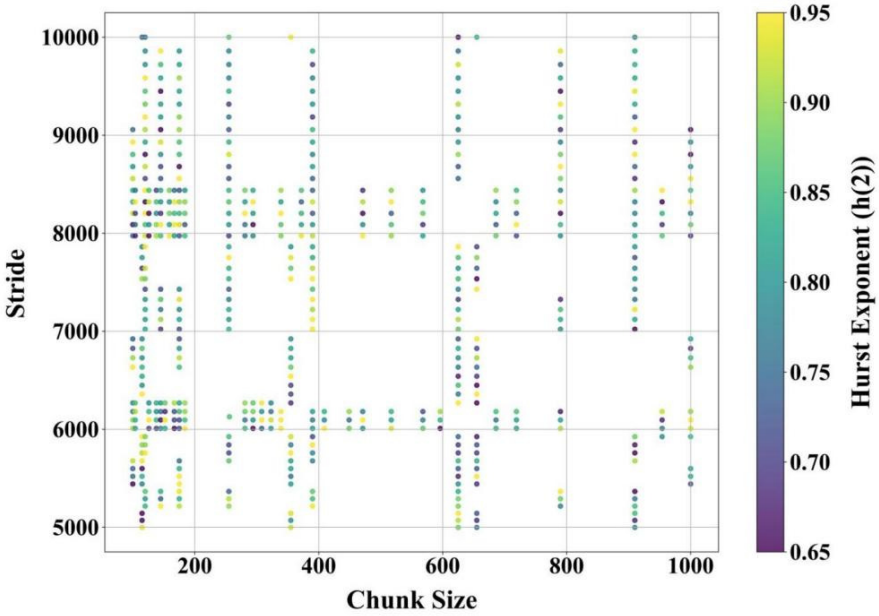


**Figure 5.** Sub-sample stability of the Hurst exponent [h(2)]. Each point represents the h(2) estimate for a specific data segment defined by its "Chunk Size" and starting "Stride". The color indicates the value of the exponent.

Third, surrogate data testing was used to statistically confirm that the observed memory is genuine and not a random consequence of the data's fat-tailed distribution. We generated 1000 surrogate series by randomly shuffling the original returns, a process that preserves the exact distribution but destroys all temporal correlations. As shown in Figure 6, the h(2) values from these shuffled series are tightly clustered around 0.5, as expected for a memoryless process. Our empirical value of 0.8634 lies far outside this distribution, confirming with high statistical significance that the observed long-range memory is a non-spurious feature of the market.

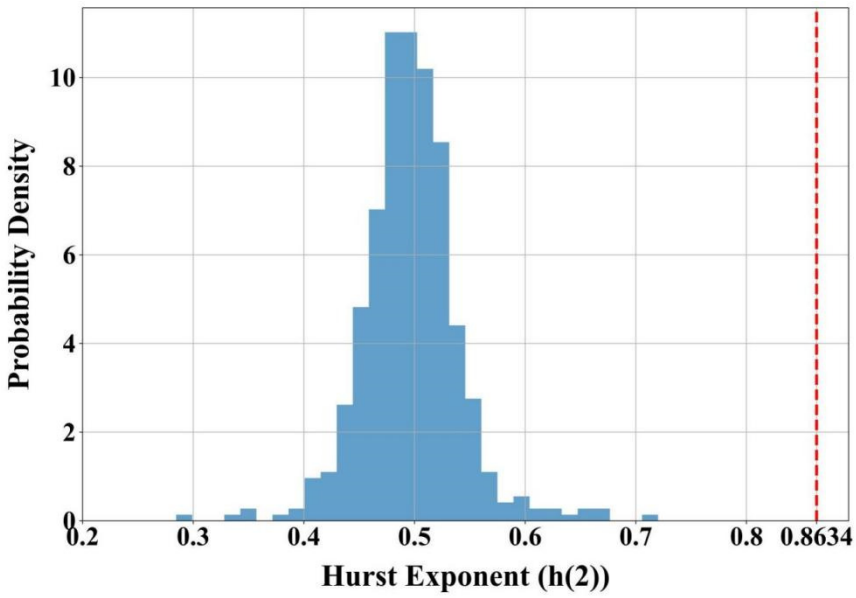


**Figure 6.** Surrogate data test for the Hurst exponent [h(2)]. The histogram shows the distribution of h(2) values from 1000 shuffled series. The red dashed line marks the h(2) value of 0.8634 from the original data.

Finally, we cross-validated the Hurst exponent estimate using three methodologically distinct estimators: MF-DFA (at q = 2), Wavelet-Leader (WL), and Local Whittle (LW). The results, shown in Table 5, demonstrate a strong consensus, with all methods pointing to significant persistence.

**Table 5.** Comparison of Hurst exponent estimates.

| Estimation method | Hurst exponent (H) Estimate |
|---|---|
| MF-DFA (q = 2) | 0.86 |
| Wavelet-Leader (WL) | 0.84 |
| Local Whittle (LW) | 0.82 |

The results in Table 5 show a strong consensus across all three methodologically distinct approaches. All estimators point to a strong and statistically significant persistence in the futures returns, with H well above the random walk benchmark of 0.5.

In summary, the combined results of our analysis provide overwhelming evidence against the weak-form efficient market hypothesis. The CSI 300 spot ETF and futures returns are characterized by non-normality, multifractality, and, most importantly, a genuine, stable, and robust long-range memory. The comprehensive set of robustness checks validates a Hurst exponent of $H \approx 0.86$. This provides a solid empirical foundation for incorporating this parameter into a more advanced pricing and arbitrage framework, as pursued in the subsequent sections.

### *4.2. Fractal futures pricing model evaluation*

#### 4.2.1. Performance of the traditional cost-of-carry model

Having established the presence of multifractal characteristics in the market returns in Section 4.1, this section empirically evaluates the performance and efficiency of the proposed fractal futures pricing model developed in Chapter 2.2.2. The primary objective is to compare its accuracy against the traditional CoC model, thereby demonstrating the practical benefits of incorporating fractal dynamics into the pricing framework.

We first revisit the traditional CoC model's performance in the context of the Chinese market. As outlined previously, traditional models often struggle due to their reliance on assumptions like random walks and market efficiency, which are frequently violated in real markets. To assess this empirically, we apply the standard CoC formula to daily closing data for the CSI 300 index (as the spot asset for pricing evaluation) and its corresponding futures contract series from March 25, 2015, to December 31, 2024. For the model parameters, we use the China 10-year government bond yield as a proxy for the risk-free rate (the latest figure/value is 1.65%) and the historical average dividend yield of the CSI 300 index (approximately 2.70%). The resulting theoretical futures prices are compared to the actual market prices, and the absolute pricing errors are calculated.

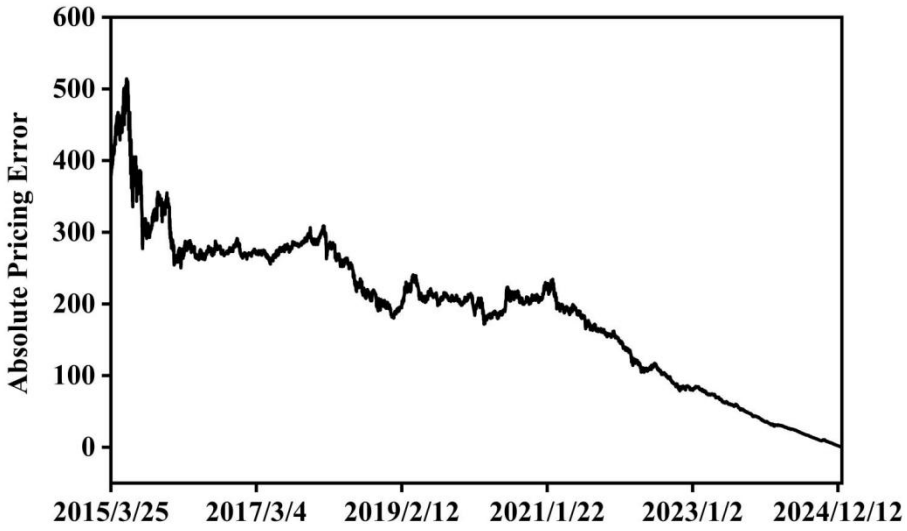


**Figure 7**. Absolute pricing error of the traditional cost-of-carry model for CSI 300 futures.

Figure 7 graphically underscores the inherent limitations of the traditional Cost-of-Carry (CoC) model when applied to the dynamic CSI 300 futures market. The plot of absolute pricing errors reveals not only considerable volatility but also a discernible pattern: deviations from actual market prices are often more substantial and erratic for contracts further from their expiration date. This observed behavior inevitably prompts a critical re-examination of the CoC model's foundational reliance on efficient market hypothesis (EMH) principles, thereby highlighting the limitations inherent in its core assumption of memoryless, random-walk price dynamics. These EMH-based assumptions, which our earlier fractal analysis suggests are frequently violated, starkly contrast with the empirically observed persistence and nonlinearities inherent in financial markets. As a result, the model's predictive power diminishes significantly when the strong anchoring effect of expiry-driven price convergence is not yet dominant. This exposes investors relying solely on this framework to considerable mispricing risk, potentially leading to flawed valuation, suboptimal hedging decisions, and inefficient capital allocation. The observed inadequacy of the traditional approach, particularly its failure to capture the complex, memory-laden structure of price movements over extended horizons, strongly motivates and validates the exploration of alternative frameworks, and consequently, the development of the proposed fractal model, which is designed to endogenously account for these market realities.

### 4.2.2. Comparative analysis of pricing accuracy

We now compare the pricing accuracy of the fractal model, which incorporates the Hurst exponent to account for long-range memory, against the traditional CoC model. Using the same dataset and period, we calculate the theoretical prices derived from the fractal pricing formula (18). Table 6 provides a snapshot comparing the actual futures prices with the theoretical prices from both models for a selected period.

**Table 6.** Comparison of actual futures prices with traditional and fractal model prices.

| Date | CSI 300 Index | Futures price | Traditional model price | Fractal model price |
|---|---|---|---|---|
| 2023-08-11 | 3,884.25 | 3,882.20 | 3837.93 | 3888.88 |
| 2023-08-14 | 3,855.91 | 3,856.80 | 3810.26 | 3860.12 |
| 2023-08-15 | 3,846.54 | 3,851.40 | 3801.11 | 3850.62 |
| 2023-08-16 | 3,818.33 | 3,821.20 | 3773.34 | 3822.25 |
| 2023-08-17 | 3,831.10 | 3,831.20 | 3786.07 | 3834.91 |
| 2023-08-18 | 3,784.00 | 3,801.60 | 3739.63 | 3787.64 |
| 2023-08-21 | 3,729.56 | 3,734.80 | 3686.15 | 3732.79 |
| 2023-08-22 | 3,758.23 | 3,761.00 | 3714.59 | 3761.37 |
| 2023-08-23 | 3,696.63 | 3,705.00 | 3653.82 | 3699.60 |
| 2023-08-24 | 3,723.43 | 3,730.00 | 3680.41 | 3724.03 |
| 2023-08-25 | 3,709.15 | 3,720.60 | 3666.40 | 3709.65 |
| 2023-08-28 | 3,752.62 | 3,757.20 | 3709.69 | 3752.81 |
| 2023-08-29 | 3,790.11 | 3,796.40 | 3746.86 | 3790.19 |
| 2023-08-30 | 3,788.51 | 3,794.00 | 3745.38 | 3788.49 |
| 2023-08-31 | 3,765.27 | 3,776.80 | 3722.51 | 3765.14 |
| 2023-09-01 | 3,791.49 | 3,796.80 | 3748.54 | 3791.26 |
| 2023-09-04 | 3,848.95 | 3,857.00 | 3805.68 | 3848.40 |
| 2023-09-05 | 3,820.32 | 3,826.20 | 3777.48 | 3819.67 |
| 2023-09-06 | 3,812.03 | 3,817.20 | 3769.39 | 3811.28 |
| 2023-09-07 | 3,758.47 | 3,761.20 | 3716.54 | 3757.63 |
| 2023-09-08 | 3,739.99 | 3,739.40 | 3698.37 | 3739.06 |
| 2023-09-11 | 3,767.54 | 3,770.00 | 3725.94 | 3766.31 |
| 2023-09-12 | 3,760.60 | 3,766.60 | 3719.18 | 3759.27 |
| 2023-09-13 | 3,736.65 | 3,739.60 | 3695.60 | 3735.23 |
| 2023-09-14 | 3,733.51 | 3,737.60 | 3692.60 | 3732.00 |
| 2023-09-15 | 3,708.78 | 3,709.40 | 3668.25 | 3707.19 |
| 2023-09-18 | 3,727.71 | 3,743.80 | 3687.29 | 3725.83 |
| 2023-09-19 | 3,720.50 | 3,736.40 | 3680.26 | 3718.53 |
| 2023-09-20 | 3,705.69 | 3,720.20 | 3665.72 | 3703.63 |
| 2023-09-21 | 3,672.44 | 3,684.00 | 3632.93 | 3670.31 |

To rigorously quantify the performance difference, we compute standard error metrics: the maximum absolute error (Max AE, representing the largest single-day deviation), the mean squared error (MSE, which heavily penalizes larger errors), and the mean absolute error (MAE, representing the average magnitude of error). Table 7 summarizes these metrics for both models.

**Table 7.** Pricing error comparison between traditional and fractal models.

| Pricing model | Max absolute error | Mean squared error | Mean absolute error |
|---|---|---|---|
| Traditional model | 45692.32 | 198.55 | 514.25 |
| Fractal model | 30817.14 | 158.85 | 384.78 |

The results in Table 7 clearly demonstrate the superior performance of the fractal pricing model across all key error metrics. The fractal model substantially reduces the Max AE to 30817.14 from the traditional model's 45692.32, a decrease of approximately 33%, indicating better control over the most extreme pricing deviations and enhanced robustness in volatile situations. This advantage is further confirmed by the MSE, which heavily penalizes larger errors. The fractal model achieves an MSE of 158.85 compared to the traditional model's 198.55, a reduction of about 20%, highlighting its effectiveness in mitigating large, costly pricing errors. Similarly, the MAE is reduced from 514.25 to 384.78, a significant improvement of roughly 25%. This signifies that the fractal model's predictions are, on average, substantially closer to the actual market prices.

To visualize the relative performance over time, Figure 8 plots the pricing errors of both the traditional and fractal models throughout the study period.

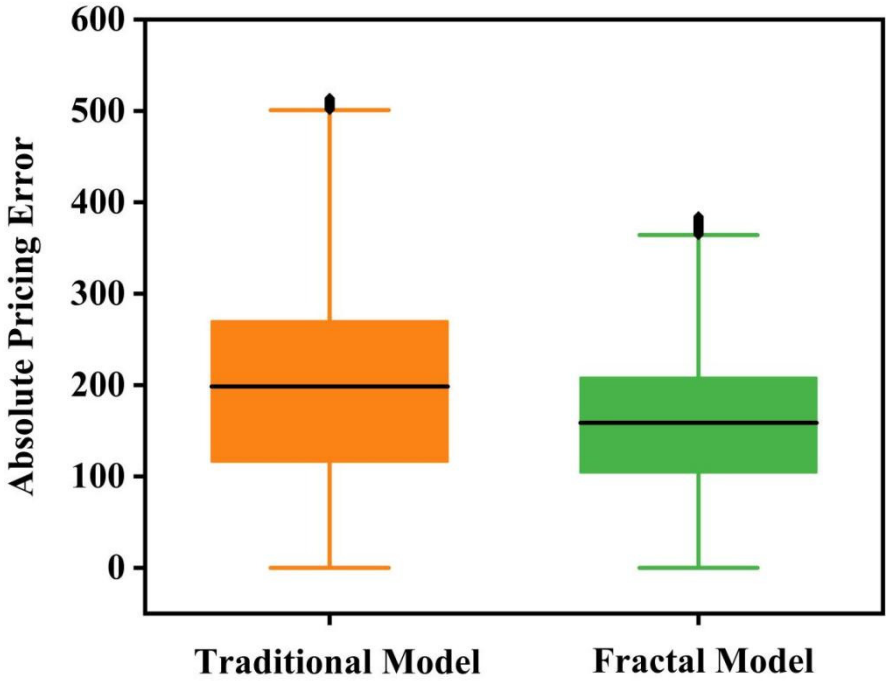


**Figure 8.** Comparison of pricing errors: traditional model versus fractal model. Each box represents the interquartile range, with the internal line marking the median. The whiskers extend to data points within 1.5 times the interquartile range, and diamond symbols indicate outliers.

Figure 8 provides a compelling visual comparison of the error distributions for the fractal and traditional models, offering clear evidence of the fractal model's advantage. The box plot for the fractal model is noticeably more compact and centered closer to zero. Its median error is lower, and its interquartile range (the box itself) is significantly tighter, indicating that the bulk of its pricing errors are far less dispersed than those of the traditional model. Furthermore, the shorter whiskers and fewer, less extreme outliers for the fractal model demonstrate its superior robustness and reduced propensity for large, erratic pricing deviations. This visual interpretation is supported by the data: empirically, the fractal model yields a lower pricing error than the traditional model on approximately 74.84% of the trading days in the sample. Collectively, these characteristics illustrate that the fractal model provides not only more accurate but also more stable and reliable price estimates. While these results strongly suggest the fractal model's superiority, it is crucial to formally test whether this improvement is statistically significant.

#### 4.2.3. Statistical validation of pricing model superiority

To address the need for formal statistical validation, we employ the Diebold–Mariano (DM) test to determine if the observed difference in predictive accuracy between the two models is statistically significant. The DM test is a standard and robust method for comparing the forecast accuracy of two competing models, making it ideal for this analysis.

The test is based on the loss differential series, defined as $d_t = L(e_{\text{trad},t}) - L(e_{\text{frac},t})$, where $L(e)$ is a loss function of the forecast error $e$. We evaluate this using two common loss functions: squared error (corresponding to MSE), where $L(e_t) = e_t^2$, and absolute error (corresponding to MAE), where $L(e_t) = |e_t|$. The null hypothesis ($H_0$) of the DM test is that both models have equal predictive accuracy, meaning the expected loss differential is zero ($E[\mathrm{d_t}] = 0$). The alternative hypothesis ($H_1$) is that the fractal model is more accurate, implying a positive expected loss differential ($E[\mathrm{d_t}] > 0$).

The DM statistic is calculated as the mean of the loss differential divided by its standard error, which is adjusted for potential autocorrelation. Under the null hypothesis, the DM statistic follows a standard normal distribution. The results of the test are presented in Table 8.

**Table 8.** Diebold–Mariano test for equal predictive accuracy.

| Loss function | DM statistic | p-value |
|---|---|---|
| Squared error (MSE) | 2.98 | < 0.01 |
| Absolute error (MAE) | 3.92 | < 0.01 |

The results of the Diebold–Mariano test are unequivocal. For both the squared error and absolute error loss functions, the DM statistics are large, positive, and highly significant. With p-values well below the 0.01 level for both tests, we can confidently reject the null hypothesis of equal predictive accuracy.

This statistical evidence confirms that the superior performance of the fractal futures pricing model is not a random occurrence. The reduction in pricing errors achieved by the fractal model is statistically significant, validating its enhanced ability to capture market dynamics compared to the traditional Cost-of-Carry model. This provides a robust quantitative foundation for the conclusion that the fractal model is a more accurate and reliable tool for futures pricing. The enhanced accuracy

and efficiency of the fractal model provide a more reliable foundation for valuation, risk management, and the development of sophisticated trading strategies, such as the optimized arbitrage strategy explored in the next section.

### *4.3. Empirical evaluation of the fractal cash-futures arbitrage strategy*

Building upon the enhanced pricing accuracy demonstrated by the fractal model, this section evaluates the performance, effectiveness, and robustness of the novel cash-futures arbitrage strategy constructed using fractal market principles. The strategy, detailed in Chapter 2.3, leverages the trend fractal dimension and momentum lifecycle theory to dynamically identify arbitrage opportunities in the basis, aiming to capture profits from basis mean-reversion, particularly during identified reversal phases.

#### 4.3.1. Basis dynamics and strategy performance

The existence and fluctuation of the basis between the spot asset (510310.SH ETF) and the CSI 300 futures contract provide the potential for arbitrage. As shown in Figure 9, the basis exhibited significant volatility during the analysis period (March 25, 2015, to December 31, 2024), oscillating roughly between −20 and +40 points. For a cash-futures arbitrage strategy, the crucial task is to determine if these deviations are large enough to yield a profit after accounting for all transaction and holding costs. A viable trading opportunity only emerges when this net basis is sufficiently positive.

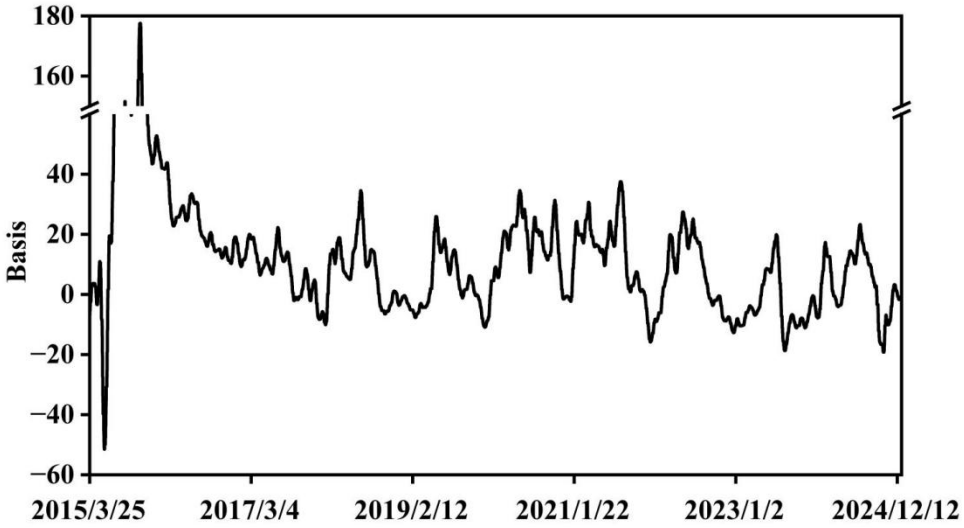


**Figure 9.** Basis for CSI 300 during the backtest period.

To ensure a robust assessment of the proposed arbitrage strategy's economic viability, a realistic transaction cost model is indispensable, particularly given the higher trading frequency inherent to the fractal approach. The ultimate performance of any arbitrage strategy is determined by its net return after deducting all execution-related expenses.

In this backtest, we assume a comprehensive round-trip transaction cost that includes commissions for both the ETF and the index futures contract, as well as an estimate for slippage. A

round-trip trade consists of opening a position (e.g., buying the ETF and selling the future) and subsequently closing it (selling the ETF and buying the future). We model the total cost as follows:

ETF costs: A commission of 0.03% (3 basis points) is charged for both the purchase and sale of the ETF.

Futures costs: A commission of 0.023% (2.3 basis points) of the notional value is applied to both opening and closing the futures position, aligning with the standard rate for intraday trading of index futures in the Chinese market.

Slippage costs: To account for execution price impact and the bid-ask spread, a conservative slippage cost of 0.01% (1 basis point) is added for each of the four legs of a complete round-trip trade (buying the ETF, selling the ETF, buying the future, and selling the future).

In aggregate, our assumed total round-trip transaction cost is approximately 0.15% of the traded value. All subsequent performance metrics, including net returns and after-cost Sharpe ratios, are calculated by deducting this cost from the gross profit of each trade. This provides a more pragmatic and rigorous perspective on the strategy's real-world potential.

We backtested the proposed fractal arbitrage strategy over this period using 5-minute frequency data. The strategy identifies potential entry points during low-basis reversal phases (buy spot, sell futures) and exit/short entry points during high-basis reversal phases (sell spot, buy futures), as determined by the FTD criteria. The key performance metrics are summarized in Table 9.

**Table 9.** Net performance of the fractal arbitrage strategy.

| Metric | Number of open trades | Number of close trades | Net total return | Net annualized return | After-cost Sharpe ratio | Maximum drawdown | Win rate |
|---|---|---|---|---|---|---|---|
| Value | 8978 | 8978 | 12.71% | 1.74% | 0.32 | 7.84% | 49.59% |

The results in Table 9 depict a strategy characterized by extremely high trading activity, executing 8978 round-trip trades over the analysis period. The strategy generated a positive net total return of 12.71%, which corresponds to a net annualized return of 1.74%. The after-cost Sharpe ratio is 0.32, indicating a positive but modest risk-adjusted return after accounting for transaction costs. The strategy experienced a maximum drawdown of 7.84%. A key observation is the win rate of 49.59%, which is slightly below the 50% break-even level. The fact that the strategy achieved a positive overall return despite a majority of trades being unprofitable suggests that the average profit from winning trades was sufficiently larger than the average loss from losing trades to overcome both the losses and transaction costs.

### 4.3.2. Comparative effectiveness analysis

To assess the effectiveness of the fractal approach, we compare its performance against a traditional cash-futures arbitrage strategy. The traditional strategy typically relies on fixed thresholds defining a "no-arbitrage band" around the theoretical futures price derived from the CoC model. Trades are triggered only when the actual basis moves outside this predetermined band. Figure 10 illustrates this concept.

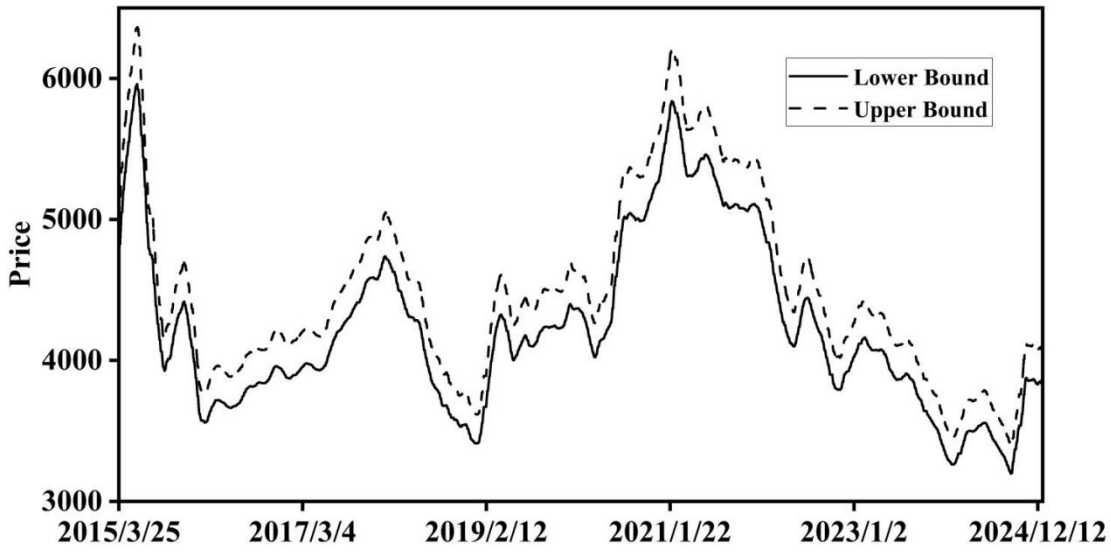


**Figure 10.** Basis for CSI 300 during the backtest period.

Table 10 directly compares the performance metrics of the fractal strategy and the traditional band-based strategy over the same backtest period.

**Table 10.** Performance comparison of arbitrage strategies.

| Metric | Number of open trades | Number of close trades | Net total return | Net annualized return | After-cost Sharpe ratio | Maximum drawdown | Win rate |
|---|---|---|---|---|---|---|---|
| Traditional strategy | 6509 | 6509 | 7.06% | 0.58% | −0.61 | 5.47% | 40.79% |
| Fractal strategy | 8978 | 8978 | 12.71% | 1.74% | 0.32 | 7.84% | 49.59% |

The comparative analysis in Table 10 starkly illuminates the superior efficacy and economic viability of the fractal-based approach. While both strategies generated positive nominal returns, the fractal strategy delivered a net total return of 12.71%, significantly outpacing the 7.06% from the traditional method, and more than tripled the net annualized return (1.74% vs. 0.58%). This performance gap is most critically underscored by the risk-adjusted returns. The fractal strategy achieved a positive after-cost Sharpe ratio of 0.32, demonstrating its ability to generate a favorable return for the risk undertaken. In stark contrast, the traditional strategy's negative Sharpe ratio of -0.61 reveals that it failed to compensate for its risk after costs, rendering it fundamentally inefficient from an investment perspective. This superior outcome was achieved through a more adaptive trading logic; the fractal strategy was more active (8978 trades vs. 6509) and, crucially, demonstrated a significantly higher win rate (49.59% vs. 40.79%). Although this dynamic approach resulted in a moderately higher maximum drawdown (7.84% vs. 5.47%), the vastly improved profitability and positive risk-adjusted performance confirm that the fractal model's ability to more precisely identify and capitalize on genuine arbitrage opportunities far outweighs the marginal increase in risk.

### 4.3.3. Stress-testing for robustness

A definitive test for any trading strategy, particularly those designed for stable returns like arbitrage, is its performance and resilience during periods of extreme, acute market distress. To assess the fractal arbitrage strategy under such severe conditions, we subject it to an analysis during what is widely regarded as the most precipitous phase of the 2015 Chinese stock market crash: the period from June 15, 2015, to July 9, 2015. This exceptionally violent 18-trading-day window witnessed an unprecedented market collapse. The Shanghai Composite Index plummeted from 5174 points to 3373 points (a 34.8% drop), the Shenzhen Component Index fell from 18,182 to 10,850 (a 40.3% decline), and the CSI 500 Index, representing core growth stocks, crashed from 11,589 to 6444 (a staggering 44.4% loss). By the close on July 8, 2139 companies (77% of the market) had seen their stock prices fall by over 30%, with 1390 companies (50%) dropping by more than 50%. Furthermore, around 1400 companies had suspended trading to avoid the carnage. This period undeniably constitutes a true "crash" scenario, providing an unparalleled stress test.


**Figure 11.** 510310.SH Price during the 2015 stress-test period.

We compared the fractal strategy's performance during these turbulent times against both the traditional arbitrage strategy and a simple buy-and-hold strategy for the underlying ETF (510310.SH). The results are summarized in Table 11.

**Table 11.** Strategy performance during the 2015 market crash.

| Metric | Number of open trades | Number of close trades | Total return | Annualized return | Sharpe ratio | Maximum drawdown | Win rate |
|---|---|---|---|---|---|---|---|
| Buy and hold | – | – | −29.79% | −99.54% | −0.76 | 37.88% | – |
| Traditional strategy | 62 | 62 | −5.82% | −59.80% | −1.06 | 16.63% | 28.57% |
| Fractal strategy | 76 | 76 | −0.83% | −12.62% | −0.59 | 7.70% | 51.56% |

The analysis during this acute stress-test period reveals the starkly different levels of resilience among the strategies. As expected, the buy-and-hold strategy was devastated, suffering a catastrophic loss of −29.79% with a maximum drawdown of 37.88%. Crucially, the traditional arbitrage strategy also failed to provide protection, generating a significant negative return of −5.82% and a large maximum drawdown of 16.63%. Its win rate collapsed to a mere 28.57% and its Sharpe ratio was deeply negative at −1.06, indicating it was unequivocally a losing proposition during the crash.

In stark and compelling contrast, the fractal strategy demonstrated exceptional robustness. While it did not escape the market turmoil completely, its total return was a nearly breakeven −0.83%. More impressively, its maximum drawdown was held to just 7.70%, less than half that of the traditional strategy and a fraction of the buy-and-hold loss. The win rate remained above 50% at 51.56%, showing its signal-generation logic remained effective even amidst chaos. While its Sharpe ratio was negative at −0.59, it was substantially better than the traditional strategy's, showcasing superior risk control relative to its peers in an extreme environment. This superior performance during the crash, achieved with higher trading activity (76 trades versus 62), underscores the fractal strategy's adaptive nature. Its ability to navigate violent price swings and preserve capital in a way that the static, threshold-based model could not, provides powerful evidence of its practical value in real-world crisis scenarios.

## 5. Conclusions

This study confronted the persistent challenge of accurately pricing futures and optimizing arbitrage strategies in modern financial markets, which are characterized by complex, nonlinear dynamics that defy traditional models. We posited that the fractal market hypothesis (FMH) provides a superior theoretical lens. By systematically investigating and operationalizing the fractal properties of China's CSI 300 index and futures market, this research developed and validated a more sophisticated framework for both pricing and trading. Our principal conclusions are as follows:

First, explicitly incorporating the market's long-range memory via the Hurst exponent leads to a statistically significant improvement in futures pricing accuracy. Our empirical analysis robustly identified strong persistence ($H \approx 0.86$) in the CSI 300 return series, a direct contradiction to the random walk assumption of the CoC model. The resulting fractal futures pricing model demonstrated marked superiority over the traditional CoC model. It reduced the mean squared error (MSE) and mean absolute error (MAE) by approximately 20% and 25%, respectively, and cut the maximum pricing deviation by over 30%. This enhanced accuracy was statistically validated by the Diebold–Mariano test, confirming that the fractal model provides a more reliable and robust foundation for valuation, risk management, and the construction of informed trading strategies.

Second, a dynamic arbitrage strategy engineered from fractal principles significantly outperforms conventional static-threshold methods in both profitability and risk control. By leveraging trend fractal dimensions ($D+$ and $D-$) and momentum lifecycle logic, our strategy adapted to the evolving structure of the basis. The backtest results are compelling: the fractal strategy delivered a net total return of 12.71%, substantially higher than the 7.06% from the traditional strategy. Critically, it achieved a positive after-cost Sharpe ratio of 0.32, indicating genuine risk-adjusted profitability, whereas the traditional strategy's Sharpe ratio was negative (−0.61), rendering it economically unviable. This superior performance was further validated in a severe stress test during the 2015 market crash. While a buy-and-hold strategy collapsed and the traditional

arbitrage strategy incurred significant losses (−5.82%), the fractal strategy demonstrated exceptional resilience, limiting its loss to a near breakeven at −0.83% and maintaining a much smaller drawdown. This robustness in extreme conditions underscores its practical value for capital preservation.

In summary, this research provides cohesive empirical evidence that moving from a linear, efficient-market perspective to a fractal one yields tangible benefits. By first constructing a more accurate pricing model that respects the market's memory and then designing an arbitrage strategy that adapts to its multi-scale dynamics, we have demonstrated a clear pathway to enhanced performance. This study offers valuable insights for investors and risk managers seeking more adaptive and profitable tools for navigating nonlinear markets. While the overall analysis period covers diverse market conditions, and our stress test during the 2015 crash (Section 4.3.3) offers a key insight into its robustness, a more granular investigation represents a valuable direction for future work. Specifically, future research should conduct detailed sub-period analyses to verify the strategy's performance consistency across a fuller spectrum of market regimes, such as prolonged bull markets and periods of sustained high versus low volatility. Such an analysis would provide deeper insights into whether the model behaves consistently or requires regime-specific calibration, complementing the initial findings of this study. Future research could extend this framework by applying it to other asset classes, integrating machine learning to refine the identification of momentum phases, or exploring its implications for optimal portfolio allocation in a multifractal environment.

## Author contributions

Xu Wu: Conceptualization, Formal analysis, Methodology, Writing–review. Yi Xiong: Writing–original draft, Writing–review & editing, Formal analysis, Visualization, Validation.

## Use of AI tools declaration

The authors used AI tools (ChatGPT and DeepSeek) for language editing and grammar review of this manuscript. The authors are fully responsible for the content of this publication.

## Conflict of interest

The authors declare no conflicts of interest.

## References

Aslam F, Aziz S, Nguyen D, et al. (2020). On the efficiency of foreign exchange markets in times of the COVID-19 pandemic. *Technol Forecast Soc Change* 161: 120261. https://doi.org/10.1016/j.techfore.2020.120261

Bian S, Serra T, Garcia P, et al. (2022) New Evidence on Market Response to Public Announcements in the Presence of Microstructure Noise. *Eur J Oper Res* 298: 785–800. https://doi.org/10.1016/j.ejor.2021.07.030

Bollerslev T, Mikkelsen H (1996). MODELING AND PRICING LONG- MEMORY IN STOCK MARKET VOLATILITY. *J Econometrics* 73: 151–184. https://doi.org/10.1016/0304-4076(95)01736-4

Brianzoni S, Campisi G (2020) Dynamical analysis of a financial market with fundamentalists, chartists, and imitators. *Chaos Soliton Fract* 130: 109434. https://doi.org/10.1016/j.chaos.2019.109434

Carchano Ó, Pardo Á (2009) Rolling over stock index futures contracts. *J Futures Markets* 29: 684–694. https://doi.org/10.1002/FUT.20373

Chiu M, Wong H (2011) Mean-variance portfolio selection of cointegrated assets. *J Econ Dyn Control* 35: 1369–1385. https://doi.org/10.1016/J.JEDC.2011.04.003

Chu Y, Hirshleifer D, Ma L (2017) The Causal Effect of Limits to Arbitrage on Asset Pricing Anomalies. *J Financ* 75: 2631–2672. https://doi.org/10.1111/jofi.12947

Cont R (2001) Empirical properties of asset returns: stylized facts and statistical issues. *Quant Financ* 1: 223–236. https://doi.org/10.1080/713665670

de Conti B, Gisin V, Yarygina I (2021) Dynamic Fractal Asset Pricing Model for Financial Risk Evaluation, In: *Risk Assessment and Financial Regulation in Emerging Markets' Banking: Trends and Prospects*, Cham: Springer International Publishing, 355–367. https://doi.org/10.1007/978-3-030-69748-8_17

Cornell B, French K (1983) Taxes and the Pricing of Stock Index Futures. *J Financ* 38: 675–694. https://doi.org/10.1111/J.1540-6261.1983.TB02496.X

Dossatayev A (2024) Deep Learning based Framework for Option Price Forecasting. 2024 IEEE 4th International Conference on Smart Information Systems and Technologies (SIST) 48: 346–351. https://doi.org/10.1109/SIST61555.2024.10629361

Engle R, Granger C (1987) Co-integration and error correction: representation, estimation and testing. *Econometrica* 55: 251–276. https://doi.org/10.2307/1913236

Fama E (1970) EFFICIENT CAPITAL MARKETS: A REVIEW OF THEORY AND EMPIRICAL WORK*. *J Financ* 25: 383–417. https://doi.org/10.1111/J.1540-6261.1970.TB00518.X

Gong W, Tian M, Yang X, et al. (2024) The option pricing problem based on the uncertain fractional volatility stock model. *Soft Comput,* 1–12. https://doi.org/10.1007/s00500-024-09663-6

Ibrahim S, Misiran M, Laham M (2020). Geometric fractional Brownian motion model for commodity market simulation. *Alex Eng J* 60: 955–962. https://doi.org/10.1016/j.aej.2020.10.023

Jiang Z, Xie W, Zhou W, et al. (2019) Multifractal analysis of financial markets: a review. *Rep Prog Phys* 82: 125901. https://doi.org/10.1088/1361-6633/ab42fb

Kantelhardt J, Zschiegner S, Koscielny-Bunde E, et al. (2002) Multifractal Detrended Fluctuation Analysis of Nonstationary Time Series. *Physica A* 316: 87–114. https://doi.org/10.1016/S0378-4371(02)01383-3

Kanzari D, Said Y (2023) A complex adaptive agent modeling to predict the stock market prices. *Expert Syst Appl* 222: 119783. https://doi.org/10.1016/j.eswa.2023.119783

Li H, Sun M, Wang Z (2024) Application of deep learning to option hedging strategy. *Syst Soft Comput* 6: 200117. https://doi.org/10.1016/j.sasc.2024.200117

Li H, Wu M, Wang X (2009) Fractional-moment Capital Asset Pricing model. *Chaos Soliton Fract* 42: 412–421. https://doi.org/10.1016/J.CHAOS.2009.01.003

Lintner J (1965) THE VALUATION OF RISK ASSETS AND THE SELECTION OF RISKY INVESTMENTS IN STOCK PORTFOLIOS AND CAPITAL BUDGETS. *Rev Econ Stat* 47: 13–37. https://doi.org/10.1016/B978-0-12-780850-5.50018-6

Lo A (2004) The Adaptive Markets Hypothesis. *J Portfolio Manage* 30: 15–29. https://doi.org/10.3905/jpm.2004.442611

Lucas A (2022) Non-equilibrium Phase Transitions in Competitive Markets Caused by Network Effects, Proceedings of the National Academy of Sciences of the United States of America, 119: e2206702119. https://doi.org/10.1073/pnas.2206702119

Mandelbrot B (1963) The Variation of Certain Speculative Prices. *J Bus* 36: 394–419. https://www.jstor.org/stable/2350970

Miao J, Yang X (2015) Pricing Model for Convertible Bonds: A Mixed Fractional Brownian Motion with Jumps. *E Asian J Appl Math* 5: 222–237. https://doi.org/10.4208/eajam.221214.240415a

Miloș L, Hațiegan C, Miloș M, et al. (2020) Multifractal Detrended Fluctuation Analysis (MF-DFA) of Stock Market Indexes. Empirical Evidence from Seven Central and Eastern European Markets. *Sustainability* 12: 535. https://doi.org/10.3390/su12020535

Nadtochiy S (2020) A Simple Microstructural Explanation of the Concavity of Price Impact. *Math Financ* 32: 78–113. https://doi.org/10.1111/mafi.12314

Peters E (1989) Fractal Structure in the Capital Markets. *Financ Anal J* 45: 32–37. https://doi.org/10.2469/FAJ.V45.N4.32.

Pohl W, Schmedders K, Wilms O (2018) Higher-order effects in asset-pricing models with long-run risks. *J Financ* 73: 1061–1111. https://doi.org/10.1111/JOFI.12615

Wu X, Chun W, Lin Y, et al. (2018) Identification of momentum life cycle stage of stock price. *Nonlinear Dynam* 94: 249–260. https://doi.org/10.1007/S11071-018-4356-1

Yan Y, Wang Y. (2022). Asset Pricing Model Based on Fractional Brownian Motion. *Fractal Fract* 6: 99. https://doi.org/10.3390/fractalfract6020099

Yousuf M, Khaliq A (2021) Partial differential integral equation model for pricing American option under multi state regime switching with jumps. *Numer Meth Part D E* 39: 890–912. https://doi.org/10.1002/num.22791

Yu P, Yan X (2019) Stock price prediction based on deep neural networks. *Neural Comput Appl* 32: 1609–1628. https://doi.org/10.1007/s00521-019-04212-x


AIMS Press